

# Improved volatile cargo retention and mechanical properties of capsules via sediment-free in situ polymerization with cross-linked poly(vinyl alcohol) as an emulsifier

Zhang, Yan; Mustapha, Abdullah; Zhang, Xiaotong; Baiocco, Dan; Wellio, Gilmore; Davies, Thomas; Zhang, Zhibing; Li, Yongliang

DOI:  
[/10.1016/j.jcis.2020.01.115](https://doi.org/10.1016/j.jcis.2020.01.115)

License:  
Creative Commons: Attribution-NonCommercial-NoDerivs (CC BY-NC-ND)

*Document Version*  
Peer reviewed version

*Citation for published version (Harvard):*  
Zhang, Y, Mustapha, A, Zhang, X, Baiocco, D, Wellio, G, Davies, T, Zhang, Z & Li, Y 2020, 'Improved volatile cargo retention and mechanical properties of capsules via sediment-free in situ polymerization with cross-linked poly(vinyl alcohol) as an emulsifier', *Journal of Colloid and Interface Science*, vol. 568, pp. 155-164.  
<https://doi.org/10.1016/j.jcis.2020.01.115>

[Link to publication on Research at Birmingham portal](#)

## General rights

Unless a licence is specified above, all rights (including copyright and moral rights) in this document are retained by the authors and/or the copyright holders. The express permission of the copyright holder must be obtained for any use of this material other than for purposes permitted by law.

- Users may freely distribute the URL that is used to identify this publication.
- Users may download and/or print one copy of the publication from the University of Birmingham research portal for the purpose of private study or non-commercial research.
- User may use extracts from the document in line with the concept of 'fair dealing' under the Copyright, Designs and Patents Act 1988 (?)
- Users may not further distribute the material nor use it for the purposes of commercial gain.

Where a licence is displayed above, please note the terms and conditions of the licence govern your use of this document.

When citing, please reference the published version.

## Take down policy

While the University of Birmingham exercises care and attention in making items available there are rare occasions when an item has been uploaded in error or has been deemed to be commercially or otherwise sensitive.

If you believe that this is the case for this document, please contact [UBIRA@lists.bham.ac.uk](mailto:UBIRA@lists.bham.ac.uk) providing details and we will remove access to the work immediately and investigate.

Download date: 25. Apr. 2024

Improved Volatile Cargo Retention and Mechanical Properties of Capsules via Sediment-Free In Situ Polymerization with Cross-Linked Poly(Vinyl Alcohol) as an Emulsifier

Yan Zhang, Abdullah Naseer Mustapha, Xiaotong Zhang, Daniele Baiocco, Gilmore Wellio, Thomas Davies, Zhibing Zhang, Yongliang Li

PII: S0021-9797(20)30130-2  
DOI: <https://doi.org/10.1016/j.jcis.2020.01.115>  
Reference: YJCIS 25988

To appear in: *Journal of Colloid and Interface Science*

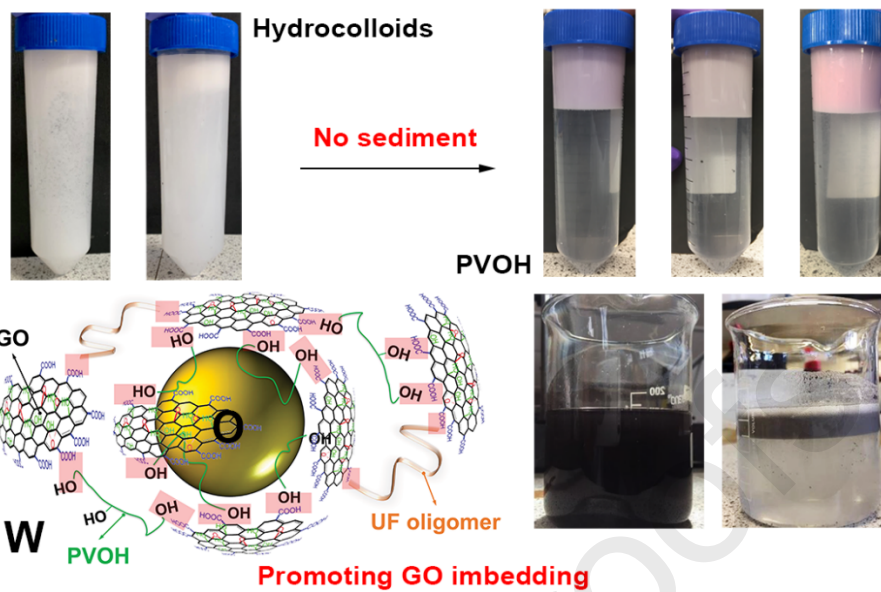
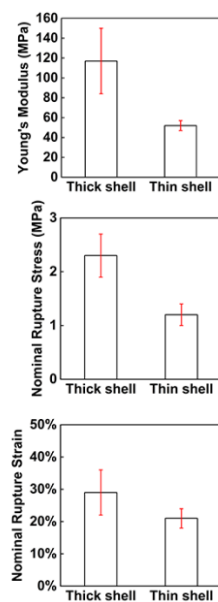
Received Date: 1 October 2019  
Revised Date: 27 January 2020  
Accepted Date: 28 January 2020

Please cite this article as: Y. Zhang, A. Naseer Mustapha, X. Zhang, D. Baiocco, G. Wellio, T. Davies, Z. Zhang, Y. Li, Improved Volatile Cargo Retention and Mechanical Properties of Capsules via Sediment-Free In Situ Polymerization with Cross-Linked Poly(Vinyl Alcohol) as an Emulsifier, *Journal of Colloid and Interface Science* (2020), doi: <https://doi.org/10.1016/j.jcis.2020.01.115>

This is a PDF file of an article that has undergone enhancements after acceptance, such as the addition of a cover page and metadata, and formatting for readability, but it is not yet the definitive version of record. This version will undergo additional copyediting, typesetting and review before it is published in its final form, but we are providing this version to give early visibility of the article. Please note that, during the production process, errors may be discovered which could affect the content, and all legal disclaimers that apply to the journal pertain.



## Improved Mechanical Properties



Graphical Abstract

**Improved Volatile Cargo Retention and Mechanical Properties of Capsules via Sediment-Free In Situ Polymerization with Cross-Linked Poly(Vinyl Alcohol) as an Emulsifier \***

Yan Zhang<sup>a,b</sup>, Abdullah Naseer Mustapha<sup>a,b</sup>, Xiaotong Zhang<sup>b</sup>, Daniele Baiocco<sup>b</sup>, Gilmore Wellio<sup>a,b</sup>, Thomas Davies<sup>c</sup>, Zhibing Zhang<sup>b\*</sup> and Yongliang Li<sup>a\*</sup>

<sup>a</sup>Birmingham Centre for Energy Storage (BCES), School of Chemical Engineering, University of Birmingham, Edgbaston, Birmingham, West Midlands, United Kingdom, B15 2TT

<sup>b</sup>Micromanipulation and Microencapsulation Research Group (MCAP), School of Chemical Engineering, University of Birmingham, Edgbaston, Birmingham, West Midlands, United Kingdom, B15 2TT

<sup>c</sup>Cardiff Catalysis Institute, School of Chemistry, Cardiff University, Cardiff, Wales, United Kingdom, CF10 3AT

Corresponding authors:

Prof. Zhibing Zhang

Dr. Yongliang Li

Email: [Z.Zhang@bham.ac.uk](mailto:Z.Zhang@bham.ac.uk)

Email: [Y.Li.1@bham.ac.uk](mailto:Y.Li.1@bham.ac.uk)

Telephone: +44 (0) 121 414 5334 \_\_\_\_\_ Telephone: +44 (0) 121 414 5135

---

\* The First Author gave a Young Investigator Perspective oral presentation at the 9th International Colloids Conference, 16-19 June 2019, Sitges, Barcelona, Spain

## Abstract

### Hypothesis

It is hypothesized that poly(vinyl alcohol) (PVOH) as an emulsifier destabilizes the insoluble molecular aggregates by increasing interparticle interactions and their tendency toward agglomeration into large particle aggregates during the encapsulation process of one-step in situ polymerization. Porosity of capsule shells is expected to decrease with reducing agglomeration tendency to allow dense packing of smaller insoluble aggregates. Cross-linking the polymer network further reduces shell permeability to improve the retention of volatile cargos. PVOH also modifies the short-range order of polymer network to bestow improved mechanical properties in addition to the shell thickening effect at appropriate synthesis conditions.

### Experiments

PVOH was used to stabilize heptane-in-water emulsions as a template for producing capsules via the one-step in situ polymerization. Shell morphologies at different PVOH concentrations were compared. Physical freeze-thawing and chemical cross-linking were adopted separately to synthesize capsules with a volatile cargo, and its retention was characterized qualitatively by a solvatochromism-based fluorescent method and quantitative payload calculation. Mechanical properties of capsules were tested with micromanipulation. The effect of GO impregnation into capsules was studied with various co-emulsifiers.

### Findings

When PVOH alone was used as the emulsifier for capsule synthesis, the higher its concentration, the more porous the shell structure was. At very low concentrations, visible pores were eliminated. Freeze-thaw cycles reduced the permeability of capsule shells when visible pores were absent. Chemical cross-linking with poly(acrylic acid) (PAA) significantly improve the retention of volatile cargo heptane. PVOH significantly reduced polymer

sediment during capsule synthesis, which eliminated the tedious centrifugation procedure that normally would have followed. Superior mechanical strength of capsules was achieved with PAA cross-linked PVOH at appropriate conditions. The impregnation of aqueously dispersed graphene oxide into capsule was also promoted by using PVOH but not hydrocolloid emulsifiers.

Keywords: capsule; emulsifier; graphene oxide; poly(vinyl alcohol); sediment; volatile.

## 1. Introduction

Encapsulation and full retention of volatile, small molecular weight active ingredients is a challenging task that remains unsolved by current technologies used in industry and academia, as most typical microcapsule membranes are highly permeable.<sup>1</sup> It is, however, very important in a wide range of areas such as personal/home care products, pharmaceuticals, foods, etc. In particular, microencapsulation of solid–liquid phase change materials (PCMs) has been recognized as a vital technology to protect them from leakage and running off and thus received tremendous attention from fundamental studies to industrial development in recent decades.<sup>2</sup> For cold thermal energy storage applications, PCMs with appropriate liquid-solid phase transition temperatures normally have high vapor pressure and low boiling points, making their encapsulation even more challenging than other applications for full retention..

Among all currently available encapsulated techniques, in situ polymerization is believed to be the most suitable method for retaining volatile PCMs due to its dense polymer structure network to prevent leakage and achieve long-term retention.<sup>3</sup> In situ polymerization is a widely used industrial method to synthesize amino resin capsules for the paper industry,<sup>4</sup> self-healing materials,<sup>5-7</sup> and thermal energy storage<sup>8,9</sup> to name a few. Such an encapsulation technique utilizes an oil-in-water (O/W) emulsion as a template and water soluble monomers

cross-link to form precipitates and deposit on the O/W interface to form polymer films encasing the oil droplets to form capsules eventually.<sup>10, 11</sup> Formed polymer precipitates not only can deposit on the O/W interface but also can disperse excessively in the aqueous phase as a side product. In case of the latter, multiple rounds of centrifugation and separation procedures are required to harvest the final capsule products, which is time-consuming and tedious. In addition, if the oil phase has a higher density than water, both capsules and precipitates would become sediment after centrifugation, posing difficulty to separate them.

In our previous work of screening emulsifiers for retaining volatile PCMs,<sup>3</sup> we tested poly(vinyl alcohol) (PVOH) as the emulsifier and preliminary result was unsuccessful. In this work, we furthered the preliminary study of using PVOH to synthesize capsules and discovered some very interesting and attractive merits of such an emulsifier. Firstly, PVOH did not seem to produce sediment during encapsulation. This eliminates the tedious repetitive routine of centrifugation and resolved the issue mentioned above. Secondly, the mechanical properties of capsules produced with PVOH were superior to those synthesized with hydrocolloids. Last but not least, impregnation of graphene oxide (GO) from the aqueous phase into capsules appears to be effective at the presence of PVOH. In order to employ such advantages of PVOH in this work, we investigate various methods to enhance the barrier property for retention of the volatile heptane. Our successful effort to improve the shell barrier properties makes PVOH a potential advantageous emulsifier candidate for capsule production using the one-step in situ polymerization route.

## **2. Materials and Methods**

### **2.1. Materials**

The following materials were purchased from Sigma-Aldrich UK: poly(vinyl alcohol) (363170,  $M_w$  13,000- 23,000, 87-89% hydrolysed), poly(acrylic acid) (306215, average

$M_v \sim 1,250,000$ ), gelatin from porcine skin (48722), xanthan gum from *Xanthomonas campestris* (Sigma-Aldrich G1253), methyl cellulose (Sigma-Aldrich M0262, viscosity 400 cP), urea (U5128, ACS reagent grade 99.0-100.5%), resorcinol (398047, ACS reagent,  $\geq 99.0\%$ ), ammonium chloride (A9434, for molecular biology,  $\geq 99.5\%$ ), formaldehyde (47608, for molecular biology, BioReagent,  $\geq 36.0\%$  in  $H_2O$ ), Nile red (72485), heptane (246654, anhydrous, 99%), and graphene oxide (GO) nanocolloids (795534, 2 mg/mL, dispersion in  $H_2O$ ).

## 2.2. Capsule synthesis

Detailed capsule synthesis was performed according to our standard protocol published elsewhere.<sup>12, 13</sup> To sum up, the aqueous phase was prepared by dissolving the emulsifier first at an appropriate concentration into 150 g deionized water, followed by dissolving 2.50 g urea, 0.25 g resorcinol and 0.25 g  $NH_4Cl$ . Gelatin was dissolved by heating to 50 °C and then maintained at the temperature under stirring for 5 min, then cooled down naturally.

Methylcellulose and xanthan gum were dissolved using high shear homogenization at 3000 rpm for 5 min and ultrasonication for 5 min for degassing air bubbles. For capsules prepared by pure PVOH, the emulsifier solution was dissolved in deionized water by heating at 90 °C for 4 h. For freeze-thawing, the emulsifier solution was frozen at -20 °C for 16 h, and then thawed at 20 °C for 8 h. 5 such freeze-thaw cycles were carried out before capsule synthesis.

When chemical cross-linking with PAA is required, 0.01% PVOH and 0.01% PAA were dissolved at 90 °C for 4 h and 12 h respectively and cooled down in air. When synthesizing capsules with GO, 5 mL GO nanocolloid was added into the prepared emulsifier solution.

The pH of all prepared solutions was adjusted to 3.5 with HCl. When fluorescent sensing was required, Nile red was dissolved in heptane via ultrasonication for 10 min prior to emulsification. Otherwise, heptane without fluorescent staining was emulsified in the aqueous phase inside a glass beaker on a Silverson high shear homogenizer at 1200 rpm for



20 min. The produced emulsion was then transferred into a 250 mL jacketed beaker connected to a water bath, and maintained under agitation at 600 rpm on a mechanical stirrer at 20 °C. 6.5 mL formaldehyde was injected into the emulsion and the beaker opening was covered with Al foil. The polymerization was initiated by heating up the circulating water to 55 °C and maintained for 4 h. The final products were centrifuged and vacuum filtered.

## 2.3. Characterization

### 2.3.1. Bright-field and fluorescent microscopy

Optical microscopy images were taken on a Leica DMRBE microscope with Motic Images Advanced 3.2. The fluorescent color of capsules under excitation was investigated on the same microscope with a CoolLED pE-300 illumination system. A H3 filter cube (BP420-490), a dichromatic mirror (510) and a suppression filter (LP 515) were applied. The blue excitation light maximum was around 460 nm.

### 2.3.2. Scanning electron microscopy

The morphological properties and shell thickness of the microcapsules were characterised using a Hitachi TM3030 Plus table-top SEM. The samples were coated with 5nm of gold, using a Quorum Q150R ES gold sputtering machine, with a pressure of 0.5 bar, and argon as the inert sputtering gas. Where shell thickness was characterized, capsules were firstly crushed with liquid nitrogen and imaged on SEM subsequently. For each thickness characterization, 10 randomly selected capsules were used and each capsule was measured at 10 different locations.

### 2.3.3. X-Ray Diffraction

A Bruker D8 Advanced diffractometer with a Cu tube (1.5418 Å) and LYNXEYE detector was used under ambient conditions. The powders were loaded into a silicon loading terminal,

and the measurement data were collected in a range of  $2\theta = 5 - 65^\circ$ , with a scanning rate of 0.8 s per step and an angular increment of  $0.01^\circ$ .

#### 2.3.4. Micromanipulation

A self-built micromanipulation system with a CCD camera was used for characterizing the mechanical properties of capsules. Details for the system configuration are described elsewhere.<sup>14</sup> Force transducers 403A and 405A (Aurora Scientific Inc., Canada) were mounted with polished glass needles. Capsules in a sample were dispensed via pipettes onto a pre-cut glass substrate which was fitted onto the system and dried to achieve dispersion. System compliance was tested 5 times and the mean was used to compensate the force transducer and stage displacements. 30 randomly selected capsules were compressed until either they broke or the maximum displacement load was reached.

#### 2.3.5. Payload and tableting

Capsule payload was characterized as follows: capsules were freshly dried and weighed. The powder weight was monitored every 24 h for the following 4 d. The powder sample was afterwards pressed into a tablet with a punch die on a Lloyd X mechanical tester (LS100 Plus) with a loading capacity of 100 kN. The samples were loaded at 80 kN at 10 mm/min for 120 s and then the force was relieved. The weight of the final tablet was recorded and the payload was calculated as (capsule weight – tablet weight)/capsule weight. Tablet samples were also prepared in this way for Raman microscopy.

#### 2.3.6. Raman microscopy

Raman spectra of samples were collected on a Renishaw inVia Qontor confocal Raman microscope with a RL785 (785 nm) diode laser and a CCD detector. Three accumulations were completed for each scan to reduce the signal to noise ratio. A  $5\times$  objective was used for

the pure GO and GO embedded capsules, with 0.5% and 0.1% laser power respectively. For the non-GO embedded capsules, a 20× objective was used with 10% laser power.

### 2.3.7. Transmission electron microscopy

Transmission electron microscopy (TEM) was performed on a JEOL JEM-2100 operating at 200 kV. TEM samples were prepared as follows: a small amount of sample was mixed with LR White resin in an Eppendorf tube overnight at 60° C until the resin set. Molded samples was sectioned using a Reichert Jung Ultra microtome and slices approx. 100 nm thick were placed onto carbon/formvar coated Cu grid. Multiple areas were analysed for each sample.

## 3. Results and Discussion

For this application, we have screen hundreds of organic chemicals with the following criteria: (1) a boiling point no lower than 90 °C; (2) a freeze point no higher than – 90 °C; (3) large enthalpy of fusion. Among all shortlisted candidate, heptane was selected as the model PCM due to its low cost and ease of commercial availability.

### 3.1. Encapsulation with pristine PVOH

Since hydroxyls can react with methylol urea,<sup>15</sup> PVOH should theoretically favor capsule formation even if not retaining the core cargo. During our preliminary emulsifier screening,<sup>12</sup> poly (vinyl alcohol) (PVOH) was unsuccessful for retaining volatile heptane, but capsules indeed formed. Further investigations on its concentration effect followed, and heptane appeared to have been sealed in when capsules were dispersed in water, indicated by a green fluorescent emission color with a fast retention indication method,<sup>13</sup> as demonstrated in Figure 1(a). In all cases encaged heptane leaked out almost immediately upon drying of capsules from the aqueous phase, manifested by a red emission color (Figure 1 (b)). The fast release of heptane upon drying insinuated that the capsule shells were highly permeable to the

volatile cargo and genuine retention of heptane was not achieved. Shell surface textures in some cases were grainy and patchy with pores residing within capsule shells, particularly at higher PVOH concentrations (Figure 1 (c)). These open pores seemed to have occluded at a lower PVOH concentration ( $\leq 0.01$  wt.%). The orange-red emission colors from Figure 1 (a), nevertheless, implied that shell permeability was still too high for any meaningful retention of the cargo even in the absence of visible pores. Figure 2 reveals the pores as viewed from inside the capsules. The grainy and patchy morphology disappeared at a PVOH concentration of 0.002 wt.% with only satellite particles being discretely lodged. However, formed capsules were extremely brittle and readily cracked or fragmented (Figure 1 (d)), again resulting in significant heptane leakage. At 0.5 wt.%, no capsules were formed, and only precipitates were observed. This implies that the concentration of PVOH was probably too high to promote the deposition of molecular and particle aggregates onto the O/W interface for shell formation. Yoshizawa et al. claimed that no capsules formed when using PVOH as the emulsifier.<sup>16</sup> Without any micrographs being provided, we presume that Yoshizawa *et al.* did not observe any capsule formation at a much higher polymeric emulsifier concentration of 3.3 wt.%, akin to our case of 0.5 wt.%. In order to form capsules with PVOH as emulsifier, a low concentration is preferred.

Soluble UF oligomers, insoluble molecular aggregates and insoluble particle aggregates co-exist in the aqueous phase during synthesis of PUF resin.<sup>17</sup> Hydroxyls may have participated in the UF polycondensation more slowly<sup>3</sup> than functional groups such as carboxyls. It may also have improved the water solubility of molecular aggregates. Accordingly, PVOH is not able to serve as effective reaction foothold to form insoluble continuous PUF shells. It would only rely on the diffusion of insoluble particle aggregates to the O/W interface and their fusion to form capsule shells. If this process, somehow, is dominated by deposition of large-sized insoluble particle aggregates onto the O/W interface, the interparticle gaps would grow

in size which manifest themselves as pores in the shell structure. When shell formation is dominated by molecular aggregates smaller in size, the polymer structure would appear smooth with less visible pores. This implies that increasing PVOH could destabilize the insoluble molecular aggregates by increasing interparticle interactions and their tendency toward agglomeration into large particle aggregates. The abundant hydroxyls and corresponding hydrogen bonding as a result could easily promote such interparticle interactions.

Even though our initial attempt to use PVOH to encapsulate volatile heptane was unsuccessful, an important finding was discovered. PVOH, surprisingly, can substantially reduce sediment, which could potentially resolve the abovementioned issues. No sediment was observed inside the rather clear infranatant (Figure 1 (e)) with naked eyes. Compared with this, the infranatant produced with either methyl cellulose (MC) or xanthan gum (XG) as the emulsifier respectively was highly turbid with numerous dispersed PUF precipitates. The sediments produced with either MC or XG were filtered, dried and weighed for calculation. The sediment/precursors ratio was calculated by dividing sediment weight by the total weight of all precursors including urea, formaldehyde, resorcinol, ammonium chloride and emulsifier. The shell/precursors ratio was calculated by dividing shell product weight by the total weight of all precursors. Table 1 lists the calculated results. No sediment could be filtered out when PVOH was used. However, the total shell product accounts for  $75.8 \pm 3.6\%$ . This observation seems to suggest that PVOH promotes precipitate deposition at the O/W interface rather than its dispersion in the aqueous continuous phase.

Table 1 sediment/precursors and shell/precursors ratios in capsule synthesis with 0.01 % XG, MC and PVOH

Emulsifier	Sediment/Precursors ratio	Shell/Precursors ratio
XG	$25.5 \pm 2.0\%$	$2.5 \pm 1.1\%$
MC	$24.5 \pm 1.6\%$	$14.9 \pm 3.1\%$
PVOH	0	$75.8 \pm 3.6\%$



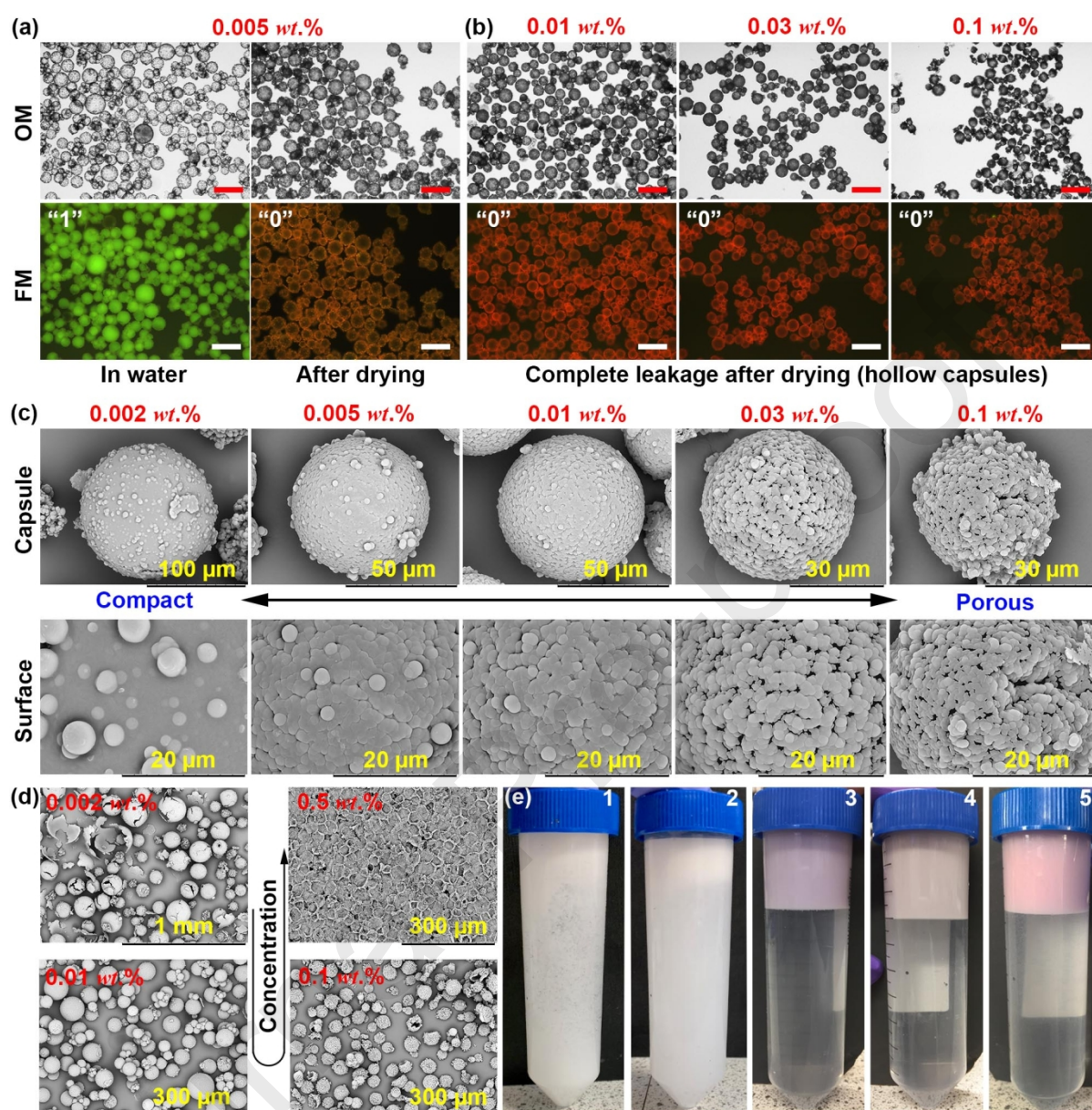


Figure 1(a) Bright-field (OM) and fluorescent microscopy (FM) images of capsules formulated with 0.005 wt.% PVOH as the emulsifier. Heptane was retained inside capsules (indicated by a green emission color, denoted as "1") when they were dispersed inside water, but escaped immediately (indicated by a red emission color, denoted as "0") upon drying. All scale bars are 100  $\mu\text{m}$ ; (b) capsules formulated with 0.01, 0.03 and 0.1 wt.% PVOH as the emulsifier showing complete heptane leakage upon drying; (c) representative surface morphology at various PVOH concentrations under scanning electron microscopy (SEM); (d) effect of PVOH concentration on capsule morphology; (e) cloudy infranatant with dispersed PUF particles and floating capsules at the top from synthesis completed with (1) 0.02 wt.% XG and (2) 0.02 wt.% MC, and clear infranatant without visible PUF particles from synthesis completed with (3) 0.01 wt.% (4) 0.03 wt.% and (5) 0.05 wt.% PVOH. All images were taken prior to centrifugation after the dispersion being allowed to settle for 5 min following being transferred from the reactor.

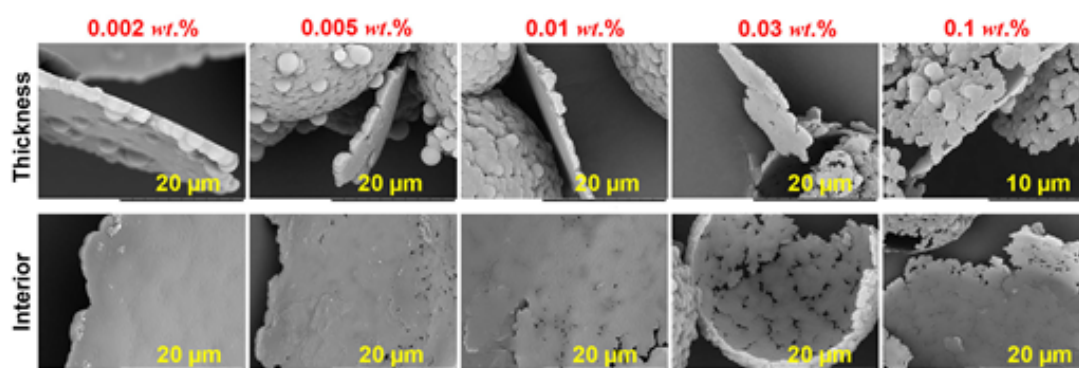


Figure 2 Thickness and interior surface morphology of capsule shells for miscellaneous PVOH concentrations

### 3.2. Encapsulation with Physically Cross-Linked PVOH via Freeze-Thawing

A significant difference in the Hansen solubility parameters (HSP) between capsule core and shell would lead to reduced shell permeability and inhibition of core diffusion.<sup>18</sup> Since heptane is a hydrocarbon and PVOH has plenty of hydroxyls, the hydrogen bonding component ( $\delta_h$ ) difference ( $\delta_{h\text{C}_7\text{H}_{16}} = 0$ ) between the shell and core is expected to be large. If the pores, functioning as pathways for small molecules to escape, are occluded within the shell polymer network, the abundant hydroxyls are expected to assist sealing heptane. Freeze-thawing cycles can physically cross-link PVOH and produce hydrogels.<sup>19-21</sup> This may increase the polymer density and reduce permeability. We therefore tested such modified PVOH as the emulsifier and results are presented in Figure 3. Physical cross-linking of PVOH dramatically improved heptane retention in capsules after drying, as opposed to immediate leakage in those synthesized with unmodified PVOH. Even though retention was still far from being practically useful, this may provide a potential solution to improve the shell barrier properties if cross-linking PVOH can alter the density of the final polymer network.

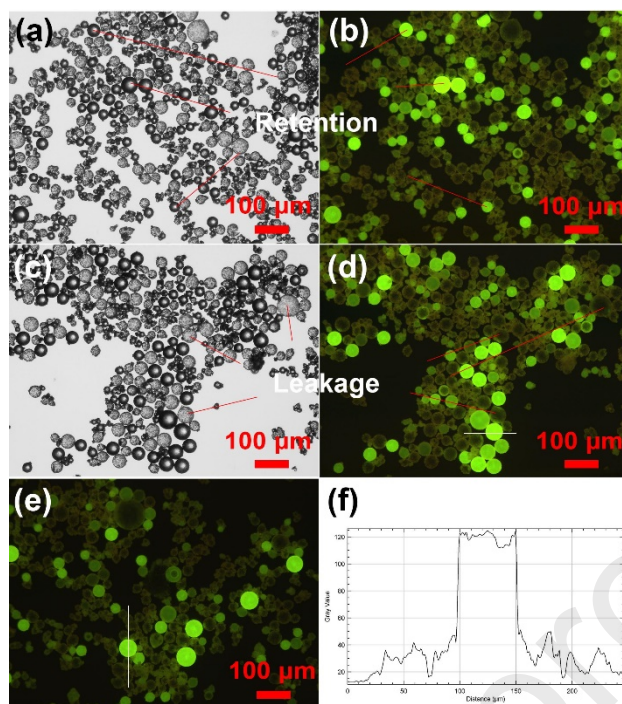


Figure 3 (a)-(d) Heptane retention/leakage inspection at two randomly selected locations by the fluorescent staining method for capsules synthesized by physically cross-linked PVOH via freeze-thawing. Images were captured immediately after capsules were freshly dried from the aqueous dispersion medium. Bright green fluorescent color indicates heptane retention while dim green color implies leakage as indicated in (a)-(d); (e)-(f) grey scale values along the white line drawn across both dim and bright fluorescent regions.

### 3.3. Encapsulation with Chemically Cross-Linked PVOH by PAA

Since physical cross-linking of PVOH reduced porosity within the PUF network created by the retardation in polycondensation by PVOH, a more effective cross-linker is expected to further improve the retention. PAA has been reported as a cross-linker for PVOH.<sup>22-25</sup> PAA would promote polycondensation by participating in the reaction with its carboxyl moieties.<sup>16</sup> A trade-off between the effects of PAA and PVOH on polycondensation,<sup>3</sup> and the cross-linking between these two molecules may be able to create a denser polymer structure to further improve capsule shell impermeability. Results in Figure 4 (a)-(d) revealed that cross-linking PVOH with PAA more successfully assisted in retaining heptane. Figure 4 (h) shows the payload evolution over 4 days after initial synthesis. Payload on the first day was calculated with the sample weight after fresh drying to be 67.5%. It should be noted,



however, that the lower payload compared with benchmark capsules produced by gelatin (GEL) ( $> 90\%$ )<sup>3</sup> may not necessarily be because of potential leakage, but the core-shell ratio. The mean shell thickness was measured to be around  $1.0 \pm 0.1 \mu\text{m}$ , as opposed to  $371 \pm 10 \text{ nm}$  for  $0.01 \text{ wt.}\%$  GEL. Payload dropped to  $39.5\%$  after 4 days, which was equivalent to  $68.6\%$  leakage. However, for capsules produced by GEL, leakage was slow and on a much smaller order of magnitude (dashed line in Figure 4 (f)). Even though the long-term retention was inferior, our experiments indeed demonstrated a gradual improvement in capsule retention capability by physically and then chemically cross-linking PVOH. This opens up opportunities of investigating other potential cross-linkers for optimum retention.

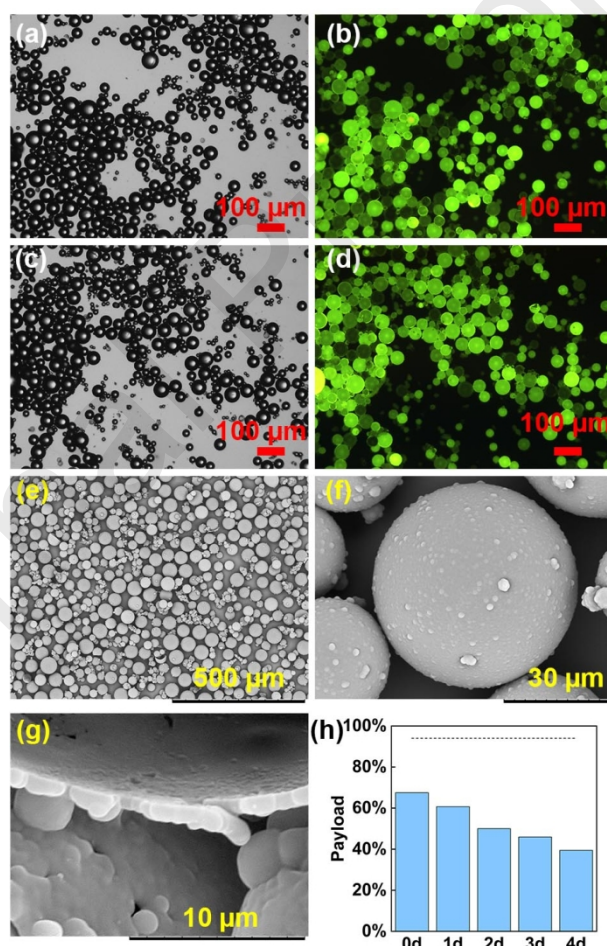


Figure 4 (a) Optical (b) fluorescence microscopy of capsules synthesized via chemically cross-linking  $0.01 \text{ wt.}\%$  PVOH with  $0.01 \text{ wt.}\%$  PAA by heating the solution at  $90^\circ\text{C}$  for 4 h. Images were captured immediately after capsules were freshly dried from the aqueous dispersion medium; (c), (d) SEM micrographs of synthesized capsules; (e) a cross section of

ruptured capsule; (f) payload of freshly dried capsules and slow leakage over 4 d. The reference dashed line represents the payload change for capsules produced with 0.01 wt.% GEL as the emulsifier.

### 3.4. Mechanical properties of capsules

Using chemically cross-linked PVOH as the emulsifier seemed to have improved the mechanical strength of capsules compared to those produced by hydrocolloids. We could hardly compress some capsules synthesized by PAA cross-linked PVOH (PVOH+PAA) during micromanipulation with the same force transducer (403A, sensitivity 0.4529 mN/V, max load 4.5 mN) used previously for characterizing capsules formed with hydrocolloids<sup>3</sup> before the maximum loading was quickly reached. A different transducer (400A, sensitivity 4.518 mN/V, max load 45 mN) was, therefore, employed. For the 30 capsules tested for each sample with either XG or MC as the emulsifier, all exhibited an ultimate failure under compression. The rupture percentage for capsules formed with GEL was 92%. However, when PVOH+PAA was used, only 14 capsules (< 50%) showed the ultimate failure point as shown in Figure 5 (a). More than 50% of the capsules exhibit no ultimate failure, but only yielding or pop-ins. Nominal rupture strain ( $29 \pm 7\%$ ) was also higher than that of their counterparts ( $25 \pm 3\%$  for GEL,  $19 \pm 2\%$  for XG and  $24 \pm 3\%$  for MC). The Young's modulus calculated by the Hertz equation<sup>26, 27</sup> was  $117 \pm 33$  MPa, which is higher than that of capsules formed with 0.01 wt.% GEL ( $19 \pm 3$  MPa), XG ( $96 \pm 12$  MPa) or MC ( $57 \pm 9$  MPa).<sup>3</sup>

X-ray diffraction (Figure 5 (d)) identified only one prominent large broad peak around  $19.2^\circ$  and an almost indiscernible one around  $42.1^\circ$  when hydrocolloids were employed as the emulsifier. Using PVOH+PAA added an additional small peak on the diffractogram around  $30.6^\circ$ . We repeated XRD with 3 different batches and this small peak consistently appeared on all diffractograms. Prominent peaks around  $31^\circ$  and  $40^\circ$  have been reported for more crystalline PUF at lower formaldehyde/urea (F/U) molar ratios  $< 1.4$ .<sup>28, 29</sup> The crystallinity for such PUF resin was calculated to be 26% at a F/U molar ratio of 1.6 and shown to decrease

with increasing F/U molar ratio.<sup>30</sup> The F/U molar ratio is approximately 2.0 in our recipe and the crystallinity would be lower. Since a single C-C bond is around 0.154 nm<sup>31</sup> and an amide bond has a length around 0.13 nm,<sup>32</sup> PUF chain lengths should be typically  $\gg 1$  nm given that the degree of polymerization (DP) of polymers would normally be  $\gg 10$ . HRTEM in Figure 6 revealed no orderly structures within capsule shells on such a length scale. It is postulated that PUF shells at least do not present long-range order. The inset in Figure 6 corresponds to the fast Fourier transform (FFT) of the highlighted areas and shows diffuse rings indicative of amorphous materials with little or no periodicity. Consequently, it is believed that PUF capsule shells are very likely amorphous. However, the new peaks on XRD diffractograms of capsule shells formed with PVOH+PAA and the less diffused ring pattern from FFT implicate that such an emulsifier may have modified the short-range order of polymer chains. It is also worth noting that the shell thickness seen in Figure 6 is in keeping with the average measurements previously determined by SEM.

Increasing Young's modulus of capsules could be caused by either increasing shell thickness from sub-microns ( $371 \pm 10$  nm for 0.01 wt.% GEL,  $823 \pm 15$  nm for 0.01 wt.% XG and  $662 \pm 12$  nm for 0.01 wt.% MC)<sup>3</sup> to  $1.0 \pm 0.1$   $\mu\text{m}$ , or modification in polymer crystallinity. We have confirmed the former with all three hydrocolloids previously.<sup>3</sup> Characterisation of the batch synthesized by cross-linking 0.01 wt.% PVOH with 0.01 wt.% PAA at 90°C for 12 h revealed that capsules had a mean shell thickness of  $267 \pm 18$  nm and the Young's modulus was  $52 \pm 5$  MPa (Figure 5 (c)).

If the different mechanical properties were entirely caused by shell thickness effect, the micrometer-shelled capsules would have been more brittle than those produced by 0.01 wt.% XG. An increasing nominal rupture strain and lowering fracture percentage of these capsules suggest improvement in shell plasticity in addition to the Young's modulus increase. The

plasticity improvement is believed to be attributed to PVOH+PAA in this case possibly via hydrogen-bonding from the abundant hydroxyls.

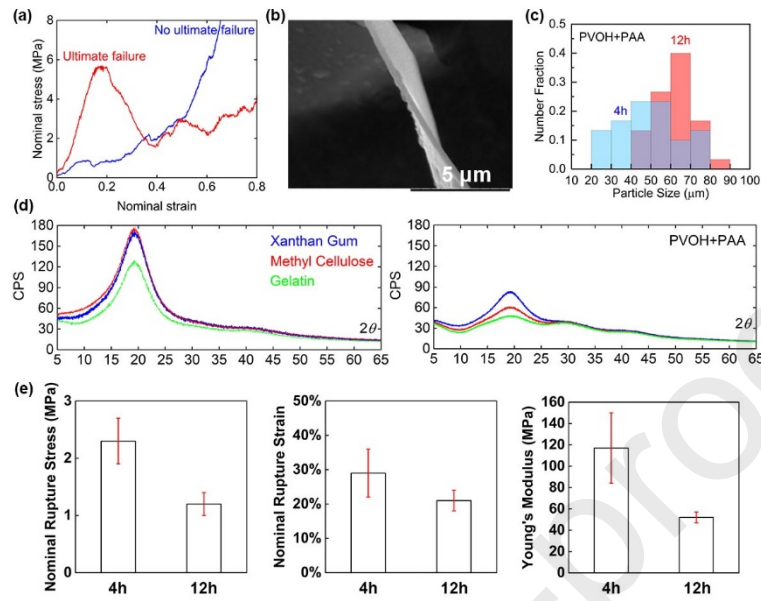


Figure 5 (a) Typical loading characteristics of capsules produced by PVOH+PAA as the emulsifier. The red curve shows capsule undergoing an ultimate failure, while the blue curve represents one exhibiting no ultimate failure but yielding and pop-ins; (b) a SEM image showing the cross section of a ruptured capsule synthesized by PVOH+PAA at 90 °C for 12 h; (c) particle size distribution of capsules synthesized by PVOH+PAA at 90 °C for 4 and 12 h; (d) x-ray diffraction (XRD) diffractogram of capsules produced by MC, XG, GEL and PVOH+PAA (3 replicates); (e) the Young's modulus, nominal rupture stress and nominal rupture strain of capsules synthesized with PVOH+PAA at 90 °C for 4 and 12 h.

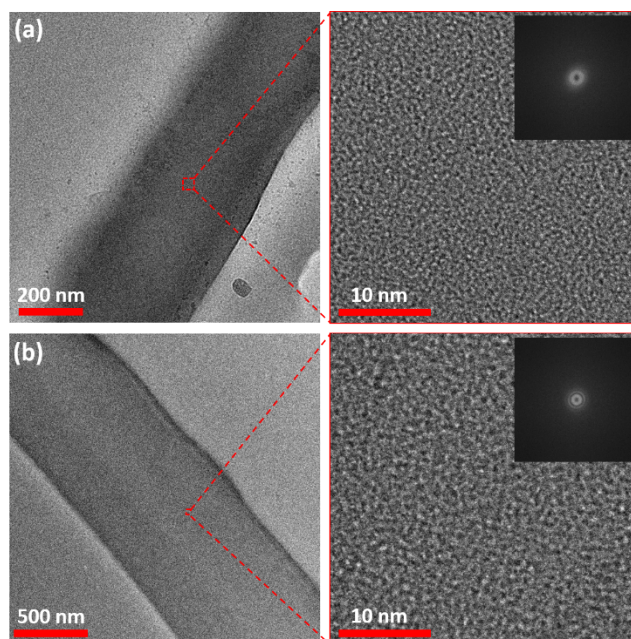


Figure 6 TEM images of PUF shells formed by using (a) GEL and (b) PVOH+PAA as an emulsifier. High resolution images of the highlighted areas are shown with the FFT inset.

### 3.5. Graphene-oxide impregnation

Another appealing advantage of using PVOH (or PVOH+PAA) emerged while we were attempting to imbue graphene oxide (GO) inside the PUF capsule shell for barrier and thermal property improvement. We dispersed GO in the aqueous phase and initiated the polymerization in order to synthesize PUF shells with GO. Surprisingly, we noticed that the majority of GO migrated into capsules after synthesis rather than being suspended in water. This was implicated by the observation that the aqueous dispersions were very dark before emulsification, while dark-colored capsules floated on the top after synthesis due to their lower density leaving the translucent infranatant without a dark tone (Figure 7 (a) and (b)). Since there was barely any sedimentation, GO did not end up as sediment either. Such a peculiar binding ability of PVOH to GO translates into a very high utilization rate of the expensive material. The shell material, PUF, with and without GO was pressed into tablets for Raman spectroscopy in order to further prove GO impregnation in capsules. PUF exhibited three large peaks at 1307, 1446 and 1625  $\text{cm}^{-1}$ , corresponding to twisting of  $(\text{CH}_2)_n$  ( $n > 3$ ), the bending of methylene in  $-\text{CH}_2-\text{OH}$ , and amide carbonyls, respectively



(Figure 7 (d)).<sup>33, 34</sup> GO showed the D band at  $1321\text{ cm}^{-1}$  and the G band at  $1608\text{ cm}^{-1}$ .<sup>35</sup> When the shell material is composed of both PUF and GO, all characteristic peaks superimposed into a single broad one.

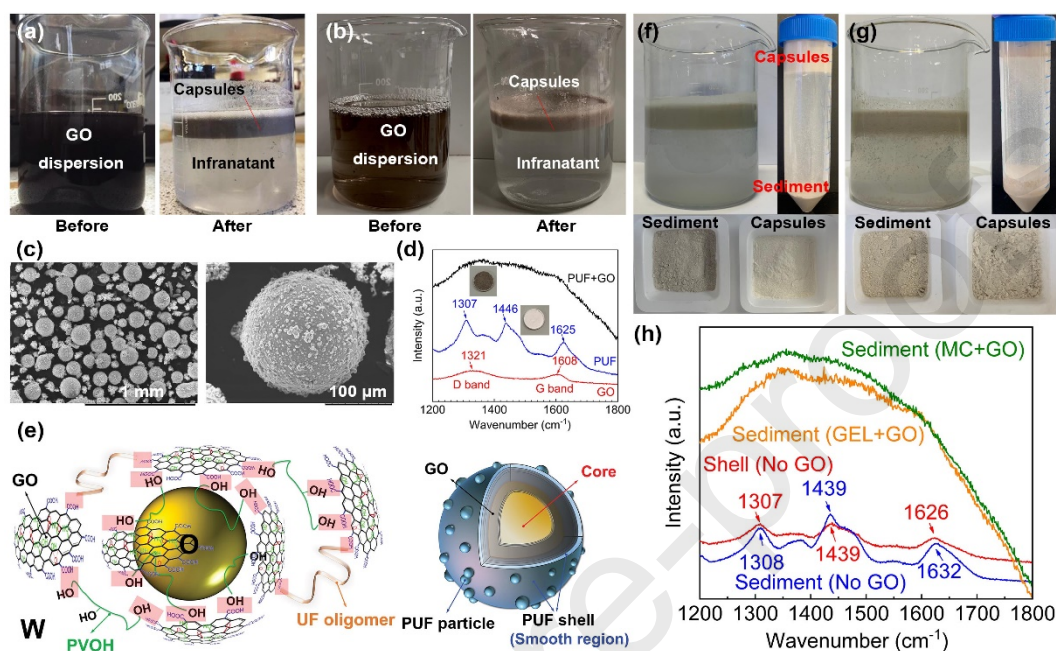


Figure 7 GO dispersion before emulsification and GO accumulation within capsules after synthesis without centrifugation with (a) 0.01 wt.% PVOH and (b) 0.01 wt.% PVOH cross-linked with 0.01 wt.% PAA as the emulsifier; (c) SEM micrographs of capsules formed with GO and 0.01 wt.% PVOH cross-linked with 0.01 wt.% PAA; (d) Raman spectra of pure GO, PUF shell and PUF+GO; (e) a schematic illustration of the intercalation between PVOH, GO and UF oligomers forming the capsule shell. Pink squares represent the cross-linking sites between GO and UF oligomers and PVOH; (f) suspension of capsules and sediment in a beaker settling for 5 min after synthesis with 0.01 wt.% GEL and GO before centrifugation; capsules on the top and sediment at the bottom of a tube after centrifugation of the suspension; dried and separated sediment and capsules; (g) suspension of capsules and sediment in a beaker settling for 5 min after synthesis with 0.01 wt.% MC and GO before centrifugation; capsules on the top and sediment at the bottom of a tube after centrifugation of the suspension; dried and separated sediment and capsules; (h) Raman spectra of PUF shell and sediment without GO, and sediment from syntheses by GEL+GO and MC+GO.

GO has shown certain amphiphilic surface activities for emulsion stabilization via a Pickering emulsion,<sup>36</sup> and would compete with PVOH for adsorption at the O/W interface.

Nevertheless, GO is believed to possess very low emulsification efficiency for nonaromatic nonpolar oils such as aliphatic hydrocarbons due to the lack of  $\pi$ - $\pi$  interactions.<sup>37</sup> PVOH, on the other hand, has a high hydrophilic-lipophilic balance (HLB) value of 18,<sup>38</sup> good for

stabilizing O/W emulsions.<sup>39</sup> Therefore, PVOH is likely to have a stronger affinity towards the O/W interface for stabilizing emulsion drops. Nevertheless, abundant hydroxyls and epoxide groups are available on its basal plane and carboxyl moieties are around the edges of the flake.<sup>40, 41</sup> Carboxyl groups have been used for cross-linking with PVOH<sup>22-25</sup> and participating in the UF polycondensation reaction.<sup>15</sup> Even though PVOH was preferentially adsorbed at the interface, GO flakes are able to migrate to the interfacial region to impregnate into PUF shell owing to its ability to cross-link with PVOH by the edge carboxyl moieties. Further cross-linking of GO within the PUF polymer network is also possible with carboxyl groups on the edges of GO reacting with the methylol group.<sup>15</sup>

For the purpose of demonstrating that this binding behavior is unique to PVOH, we tested GEL and MC as the co-emulsifier with GO. Both batches of syntheses produced sediment, contrary to when PVOH was used (Figure 7 (f) and (g)). We compared the colors between dried capsules and sediment. For the batch formulated with MC, the colors of both capsules and sediment appeared to be similar, which implied that GO could be present in both. When GEL was used, the color of sediment was darker than capsules, indicating that GO might be predominantly imbedded inside sediment rather than in capsules. Raman spectra of sediment in Figure 7 (h) confirmed that GO were indeed present in sediment for both batches.

#### **4. Conclusions and Future Perspectives**

In this work, we succeeded in using PVOH as an emulsifier<sup>12, 16</sup> for encapsulating a challenging volatile cargo via a one-step in situ polymerization. Even though PVOH was crosslinked by carboxylic groups to make retention possible, previous effort has demonstrated that carboxyl or anhydride moieties are not necessary<sup>3, 12</sup> as opposed to the prevalent usage of carboxyl-bearing emulsifiers.<sup>6, 16, 33, 42-45</sup> If there is no chemical reaction between the emulsifier and monomers, or the reaction rate is low, preferentially adsorbed

emulsifiers could not expand a continuous shell growth from chemical reactions initiating from such functional groups. Shell formation is predominantly determined by diffusion of insoluble particle aggregates onto the O/W interface. When such aggregates grow to a certain size range, shell structures become porous due to interparticle gaps. In order to retain volatile cargos with PVOH, a low concentration is preferred with a crosslinker promoting chemical reactions. Crosslinking the polymer network would close pores and increase its density to block leakage of small molecules. The most significant merit of using PVOH as the emulsifier to synthesize capsules is the substantial reduction of PUF precipitates usually produced during in situ polymerization, which eliminates the need for centrifugation to harvest capsules. Such an improvement foresees a huge industrial benefit in terms of reducing production time and simplifying manufacturing procedures. Meanwhile, capsules produced with the PVOH emulsifier also demonstrate stronger mechanical properties in terms of Young's modulus and nominal rupture strain. This is likely caused by thicker shells and a localized short-range order change. Interestingly, we also discovered that PVOH facilitated binding of GO into capsules likely owing to its binding abilities via chemical reactions. This features a high utilization efficiency of the expensive functional materials. In order to validate the hypothesis from a chemical reaction point of view, reaction rates of various functional groups such as carboxyls, hydroxyls, amines and amides in the UF polycondensation should be studied.

## **5. Acknowledgement**

The authors give their special thanks to the Engineering and Physical Sciences Research Council (EPSRC) in the United Kingdom for the funding provided to this project (EP/N000714/1 and EP/N021142/1). The authors would like to thank Mrs Theresa Morris from the School of Metallurgy and Materials at the University of Birmingham for TEM



sample preparation, as well as the Cardiff University electron microscopy facility for the TEM experiments completed.

## 6. References

1. Hitchcock, J. P.; Tasker, A. L.; Baxter, E. A.; Biggs, S.; Cayre, O. J., Long-Term Retention of Small, Volatile Molecular Species within Metallic Microcapsules. *ACS Applied Materials & Interfaces* **2015**, *7* (27), 14808-14815.
2. Liu, H.; Wang, X.; Wu, D., Innovative design of microencapsulated phase change materials for thermal energy storage and versatile applications: a review. *Sustainable Energy & Fuels* **2019**, *3* (5), 1091-1149.
3. Zhang, Y.; Baiocco, D.; Mustapha, A. N.; Zhang, X.; Qinghua, Y.; Wellio, G.; Zhang, Z.; Li, Y., Hydrocolloids: Nova Materials Assisting Encapsulation of Volatile Phase Change Materials for Cryogenic Energy Transport and Storage. *Chemical Engineering Journal* **2020**, *382*, 123028.
4. Dietrich, K.; Herma, H.; Nastke, R.; Bonatz, E.; Teige, W., Amino resin microcapsules. I. Literature and patent review. *Acta Polymerica* **1989**, *40* (4), 243-251.
5. Brown, E. N.; White, S. R.; Sottos, N. R., Microcapsule induced toughening in a self-healing polymer composite. *Journal of Materials Science* **2004**, *39* (5), 1703-1710.
6. Blaiszik, B. J.; Caruso, M. M.; McIlroy, D. A.; Moore, J. S.; White, S. R.; Sottos, N. R., Microcapsules filled with reactive solutions for self-healing materials. *Polymer* **2009**, *50* (4), 990-997.
7. Nesterova, T.; Dam-Johansen, K.; Kiil, S., Synthesis of durable microcapsules for self-healing anticorrosive coatings: A comparison of selected methods. *Progress in Organic Coatings* **2011**, *70* (4), 342-352.
8. Chen, Z.; Wang, J.; Yu, F.; Zhang, Z.; Gao, X., Preparation and properties of graphene oxide-modified poly(melamine-formaldehyde) microcapsules containing phase change material n-dodecanol for thermal energy storage. *Journal of Materials Chemistry A* **2015**, *3* (21), 11624-11630.
9. Fang, G.; Li, H.; Yang, F.; Liu, X.; Wu, S., Preparation and characterization of nano-encapsulated n-tetradecane as phase change material for thermal energy storage. *Chemical Engineering Journal* **2009**, *153* (1), 217-221.
10. Nguon, O.; Lagurné-Labarthe, F.; Brandys, F. A.; Li, J.; Gillies, E. R., Microencapsulation by in situ Polymerization of Amino Resins. *Polymer Reviews* **2017**, 1-50.
11. Sliwka, W., Microencapsulation. *Angewandte Chemie International Edition in English* **1975**, *14* (8), 539-550.
12. Zhang, Y.; Jiang, Z.; Zhang, Z.; Ding, Y.; Yu, Q.; Li, Y., Polysaccharide assisted microencapsulation for volatile phase change materials with a fluorescent retention indicator. *Chemical Engineering Journal* **2019**, *359*, 1234-1243.
13. Zhang, Y.; Zhang, Z.; Ding, Y.; Pikramenou, Z.; Li, Y., Converting Capsules to Sensors for Nondestructive Analysis: from Cargo-Responsive Self-Sensing to Functional Characterization. *ACS Applied Materials & Interfaces* **2019**, *11* (9), 8693-9642.
14. Zhang, Z., Mechanical strength of single microcapsules determined by a novel micromanipulation technique. *Journal of Microencapsulation* **1999**, *16* (1), 117-124.
15. Peker-Baslara, S.; Övez, B.; Balcioglu, Ö., Properties of gelatin-gum arabic coacervates composited with amino resins. *Journal of Chemical Technology & Biotechnology* **1993**, *56* (2), 175-184.
16. Yoshizawa, H.; Kamio, E.; Kobayashi, E.; Jacobson, J.; Kitamura, Y., Investigation of alternative compounds to poly(E-MA) as a polymeric surfactant for preparation of microcapsules by phase separation method. *Journal of Microencapsulation* **2007**, *24* (4), 349-357.

17. Ferra, J. M. M.; Mendes, A. M.; Costa, M. R. N.; Carvalho, L. H.; Magalhães, F. D., A study on the colloidal nature of urea-formaldehyde resins and its relation with adhesive performance. *Journal of Applied Polymer Science* **2010**, *118* (4), 1956-1968.
18. Hofmeister, I.; Landfester, K.; Taden, A., Controlled Formation of Polymer Nanocapsules with High Diffusion-Barrier Properties and Prediction of Encapsulation Efficiency. *Angewandte Chemie International Edition* **2015**, *54* (1), 327-330.
19. Hassan, C. M.; Peppas, N. A., Structure and Morphology of Freeze/Thawed PVA Hydrogels. *Macromolecules* **2000**, *33* (7), 2472-2479.
20. Ricciardi, R.; Auriemma, F.; De Rosa, C., Structure and Properties of Poly(vinyl alcohol) Hydrogels Obtained by Freeze/Thaw Techniques. *Macromolecular Symposia* **2005**, *222* (1), 49-64.
21. Holloway, J. L.; Lowman, A. M.; Palmese, G. R., The role of crystallization and phase separation in the formation of physically cross-linked PVA hydrogels. *Soft Matter* **2013**, *9* (3), 826-833.
22. Gudeman, L. F.; Peppas, N. A., Preparation and characterization of pH-sensitive, interpenetrating networks of poly(vinyl alcohol) and poly(acrylic acid). *Journal of Applied Polymer Science* **1995**, *55* (6), 919-928.
23. Kumeta, K.; Nagashima, I.; Matsui, S.; Mizoguchi, K., Crosslinking reaction of poly(vinyl alcohol) with poly(acrylic acid) (PAA) by heat treatment: Effect of neutralization of PAA. *Journal of Applied Polymer Science* **2003**, *90* (9), 2420-2427.
24. Gaddy, G. A.; Korchev, A. S.; McLain, J. L.; Slaten, B. L.; Steigerwalt, E. S.; Mills, G., Light-Induced Formation of Silver Particles and Clusters in Crosslinked PVA/PAA Films. *The Journal of Physical Chemistry B* **2004**, *108* (39), 14850-14857.
25. Byun, H.; Hong, B.; Nam, S. Y.; Jung, S. Y.; Rhim, J. W.; Lee, S. B.; Moon, G. Y., Swelling behavior and drug release of poly(vinyl alcohol) hydrogel cross-linked with poly(acrylic acid). *Macromolecular Research* **2008**, *16* (3), 189-193.
26. Johnson, K. L., *Contact Mechanics*. Cambridge University Press: Cambridge, United Kingdom, 1985.
27. Kuo-Kang, L., Deformation behaviour of soft particles: a review. *Journal of Physics D: Applied Physics* **2006**, *39* (11), R189.
28. Park, B.-D.; Jeong, H.-W., Hydrolytic stability and crystallinity of cured urea-formaldehyde resin adhesives with different formaldehyde/urea mole ratios. *International Journal of Adhesion and Adhesives* **2011**, *31* (6), 524-529.
29. Liu, M.; Thirumalai, R. V. K. G.; Wu, Y.; Wan, H., Characterization of the crystalline regions of cured urea formaldehyde resin. *RSC Advances* **2017**, *7* (78), 49536-49541.
30. Park, B.-D.; Causin, V., Crystallinity and domain size of cured urea-formaldehyde resin adhesives with different formaldehyde/urea mole ratios. *European Polymer Journal* **2013**, *49* (2), 532-537.
31. Bartell, L. S., On the Length of the Carbon-Carbon Single Bond<sup>1</sup>. *Journal of the American Chemical Society* **1959**, *81* (14), 3497-3498.
32. Allen, F. H.; Kennard, O.; Watson, D. G.; Brammer, L.; Orpen, A. G.; Taylor, R., Tables of bond lengths determined by X-ray and neutron diffraction. Part 1. Bond lengths in organic compounds. *Journal of the Chemical Society, Perkin Transactions 2* **1987**, (12), S1-S19.
33. Cosco, S.; Ambrogio, V.; Musto, P.; Carfagna, C., Properties of poly(urea-formaldehyde) microcapsules containing an epoxy resin. *Journal of Applied Polymer Science* **2007**, *105* (3), 1400-1411.
34. Larkin, P., Chapter 6 - IR and Raman Spectra-Structure Correlations: Characteristic Group Frequencies. In *Infrared and Raman Spectroscopy*, Elsevier: Oxford, 2011; pp 73-115.
35. Giuliadori, A. M.; Brandi, A.; Kotla, S.; Perrozzi, F.; Gunnella, R.; Ottaviano, L.; Spurio, R.; Fabbretti, A., Development of a graphene oxide-based assay for the sequence-specific detection of double-stranded DNA molecules. *PLOS ONE* **2017**, *12* (8), e0183952.

36. Kim, F.; Cote, L. J.; Huang, J., Graphene Oxide: Surface Activity and Two-Dimensional Assembly. *Advanced Materials* **2010**, 22 (17), 1954-1958.
37. He, Y.; Wu, F.; Sun, X.; Li, R.; Guo, Y.; Li, C.; Zhang, L.; Xing, F.; Wang, W.; Gao, J., Factors that Affect Pickering Emulsions Stabilized by Graphene Oxide. *ACS Applied Materials & Interfaces* **2013**, 5 (11), 4843-4855.
38. Xu, Q.; Crossley, A.; Czernuszka, J., Preparation and characterization of negatively charged poly(lactic-co-glycolic acid) microspheres. *Journal of Pharmaceutical Sciences* **2009**, 98 (7), 2377-2389.
39. Zheng, Y.; Zheng, M.; Ma, Z.; Xin, B.; Guo, R.; Xu, X., 8 - Sugar Fatty Acid Esters. In *Polar Lipids*, Ahmad, M. U.; Xu, X., Eds. Elsevier: 2015; pp 215-243.
40. Cai, W.; Piner, R. D.; Stadermann, F. J.; Park, S.; Shaibat, M. A.; Ishii, Y.; Yang, D.; Velamakanni, A.; An, S. J.; Stoller, M.; An, J.; Chen, D.; Ruoff, R. S., Synthesis and Solid-State NMR Structural Characterization of <sup>13</sup>C-Labeled Graphite Oxide. *Science* **2008**, 321 (5897), 1815-1817.
41. Compton, O. C.; Dikin, D. A.; Putz, K. W.; Brinson, L. C.; Nguyen, S. T., Electrically Conductive "Alkylated" Graphene Paper via Chemical Reduction of Amine-Functionalized Graphene Oxide Paper. *Advanced Materials* **2010**, 22 (8), 892-896.
42. Brown, E. N.; Kessler, M. R.; Sottos, N. R.; White, S. R., In situ poly(urea-formaldehyde) microencapsulation of dicyclopentadiene. *Journal of Microencapsulation* **2003**, 20 (6), 719-730.
43. Yoshizawa, H.; Kamio, E.; Hirabayashi, N.; Jacobson, J.; Kitamura, Y., Membrane formation mechanism of cross-linked polyurea microcapsules by phase separation method. *Journal of Microencapsulation* **2004**, 21 (3), 241-249.
44. Fan, C.; Zhou, X., Effect of emulsifier on poly(urea-formaldehyde) microencapsulation of tetrachloroethylene. *Polymer Bulletin* **2011**, 67 (1), 15-27.
45. Cosco, S.; Ambrogi, V.; Musto, P.; Carfagna, C., Urea-Formaldehyde Microcapsules Containing an Epoxy Resin: Influence of Reaction Parameters on the Encapsulation Yield. *Macromolecular Symposia* **2006**, 234 (1), 184-192.